Thermochimica Acta 512 (2011) 34–39

Contents lists available at ScienceDirect

Thermochimica Acta

journal homepage: www.elsevier.com/locate/tca

Thermal and electrical conduction behavior of alumina and multiwalled carbon nanotube incorporated poly(dimethyl siloxane)

Jinho Hong [a], Jeongwoo Lee [a], Dongsoo Jung [b], Sang Eun Shim [a,*]

[a] Department of Chemical Engineering, Inha University, 253 Yonghyundong, Namgu, Incheon 402-751, Republic of Korea
[b] Department of Mechanical Engineering, Inha University, 253 Yonghyundong, Namgu, Incheon 402-751, Republic of Korea

ARTICLE INFO

Article history:
Received 25 April 2010
Received in revised form 20 August 2010
Accepted 23 August 2010
Available online 18 September 2010

Keywords:
Poly(dimethyl siloxane)
Thermal conductivity
Carbon nanotube
Alumina
Electrical conductivity

ABSTRACT

Alumina particles were incorporated in poly(dimethyl siloxane) (PDMS) matrix in company with multiwalled carbon nanotube (MWCNT) for improving the thermal and electrical conductivities. The concentration of MWCNT was increased from 0 to 10 wt% to PDMS at fixed amounts of alumina (200 and 300 wt% to PDMS). Thermal conductivity of PDMS composites was increased with the increasing amount of MWCNT and the excellent dispersibility of the incorporated pristine MWCNT was achieved. Thermal and electrical conductivities of the composites were increased with the increasing concentration of the alumina because the alumina particles help disperse MWCNT within the PDMS matrix due to the ball milling effect during compounding. The properties of the alumina and MWCNT incorporated PDMS composites were investigated in terms of the curing characteristics, electrical conductivity, and thermal conductivity. The MWCNT/alumina incorporated composite showed the high electrical conductivity to the level of the semiconductor.

1. Introduction

As the conducting filler, carbon nanotube (CNT) is widely used not only for enhancing the conducting behavior but also for reinforcing the mechanical properties of composites. Since the CNT shows the extremely high thermal and electrical conductivity, and mechanical strength, a great attention has been paid to the application of CNT in electronics [1–4]. As the electronic devices need multifunction and high performance in a limited size, the thermal management of products has become more important. For example, a small difference in operating temperature in the order of 10–15 °C can result in a two-fold reduction in the life time of a device [5]. CNT has the one-dimensional unique structure which enables the composites filled with CNT to have low percolation threshold concentrations [6,7]. By using these characteristics, CNT incorporated composites show the enhancement of thermal conductivity even at low concentrations [8–10].

Many researchers have been used the metal oxides, metal and ceramics such as alumina (Al_2O_3), diamond, silicon carbide (SiC), and the zinc oxide (ZnO) as the thermal dissipative filler in the composite materials [11]. Goh et al. prepared the Al_2O_3 and ZnO filled silicone rubber where about 70% of the thermal conductivity enhancement was achieved at 10 vol% of the filler loading [12]. Kou et al. explored the effect of the particle size of alumina on the thermal conductivity of silicone rubber. Thermal conductivity of the prepared composite was improved with alumina particles with a smaller diameter at the same volume fraction [13]. Kim et al. reported the linear increase of thermal conductivity of water and ethylene glycol containing the alumina, zinc oxide, and titanium dioxide. [14]. The improvement of thermal conductivity has been explored for various systems including boron nitride (BN) in polyethylene matrix, ZnO in silicone rubber, metal oxide fillers in ethylene vinyl acetate (EVA) for the solar cell, modified ZnO in EVA, and ZnO in ethylene glycol [15–19]. Silicone rubber-based thermal interface materials with nanofillers have been widely used in industrial applications including power supplies, automotive electronics, motor controls, and power semiconductors due to their weather resistance, impact resistance, unusual flexibility, easy processing, chemical resistance, and temperature resistance [20].

The thermal conductivity of the CNT incorporated composites was also explored for their unique one-dimensional structure. Fan et al. showed the tremendous effect of CNT alignment on the thermal conductivity. When the CNT was aligned in a single direction, the composite material showed the excellent thermal conduction behavior [21]. They also reported the length effect of CNT where the thermal conductivity was the highest when the length of CNT was shortened below 1 μm [22]. Also, it has been found that the thermal conductivity of acid-purified CNT-loaded composites was higher than that of pristine CNT [23]. This effect of the purification and dispersions of CNT on the thermal conductivity of polymer

* Corresponding author. Tel.: +82 32 860 7475; fax: +82 32 872 0959.
E-mail address: seshim@inha.ac.kr (S.E. Shim).

0040-6031/$ – see front matter © 2010 Elsevier B.V. All rights reserved.
doi:10.1016/j.tca.2010.08.019

composites have been investigated by several researchers [24–28]. As discussed above, the enhancement of the thermal conductivity of polymer composites using CNT is an attractive research area.

In this work, alumina was incorporated together with the pristine MWCNT in poly(dimethyl siloxane) (PDMS; silicone rubber) matrix. The fabricated PDMS composites showed much improved thermal conductivity and electrical conductivity. Incorporated alumina particles induce the dispersive mixing of CNT by means of high shear generated among the alumina particles. With the high loading of alumina, CNT was spatially well distributed in the interstitial space to easily form the thermal and electrical conduction pathways. Curing behavior and the rheological properties were also investigated.

2. Experimental

2.1. Materials

PDMS (Mw = 674,000 g/mol, 0.1 mol% vinyl group) was supplied from KCC Co., Korea. MWCNT (Hanwha Nanotech Co. Ltd., Korea) synthesized via a chemical vapor deposition (CVD) method has more than 95% purity. The diameter of MWCNT was 10–50 nm and the length was 10–50 μm, respectively. The aspect ratio was approximately 1000. Two kinds of alumina (DAW-10 and DAW-45) purchased from Denka Co., Japan, have the median diameter of 10 and 45 μm, respectively. 2,5-Bis(tert-butylperoxy)-2,5-dimethylhexane (DHBP; Akzo Nobel, The Netherlands) was as a curative.

2.2. Compounding

The compounding of PDMS was accomplished by using a planetary mixer (PTD-001, DNTEK Co. Ltd., S. Korea) and a two-roll mill. Aluminas with 10 and 45 μm in diameters were first mixed with a 1/1 (w/w) ratio. Then the appropriate amount of the pristine MWCNT was mixed with the alumina for the distributive mixing. 100 g of PDMS was charged into the chamber of the planetary mixer. The each one third of the filler was added in every 30 min at 30 rpm. After the incorporation of all amounts of the fillers, the rotation speed of the impeller was increased from 30 to 100 rpm, then kept for 3 h at room temperature. After the additional mixing at 30 rpm for 1 h, the compound was discharged and roll-milled for 3 min prior to vulcanization. Compounded PDMS was additionally roll-milled with 1 wt% DHBP to PDMS. After the incorporation of the curing agent, the uncured composite was placed on the mold and vulcanized at 170 °C for 10 min using a hot press. The pressure of the press was 17.2 MPa.

2.3. Characterization

A scanning electron microscopy (SEM) (S-4300, Hitachi) was used to observe the morphology of MWCNT and prepared composites. In order to investigate the dispersibility and the wettability of MWCNT and alumina in the PDMS matrix, the prepared PDMS composite was cryogenically fractured. Thermal conductivity of prepared silicone pads was measured using QTM-500 (Kyoto Electronics, Japan). QTM-500 measures the thermal conductivity of thick and thin samples quickly by employing a hot wire method. When the electric power is applied to the heating wire, the temperature of wire rises with the time. Then the thermal conductivity is given by

$$\lambda = \frac{q \cdot \ln(t_2/t_1)}{4\pi(T_2 - T_1)}$$

where λ refers to the thermal conductivity of the sample and q is the generated heat per unit length. T and t are the temperature and time, respectively. Curing and rheology tests were performed on a Rubber Process Analyzer (RPA 2000, Alpha Technologies, USA) by following ASTM D6204-99. In order to remove adsorbed water in the compounds, the uncured compounds without the curative were dried at 80 °C for 24 h in the vacuum oven prior to the rheological test. It is noted that the adsorbed moisture is vaporized during the measurement in the hot biconical die, resulting in misleading data. The electrical conductivity of the composites was determined by a resistivity meter (Loresta-GP, Mitsubishi Chemical Co., Japan).

Table 1
Thermal conductivity of alumina and MWCNT incorporated PDMS composites.

MWCNT (wt% to PDMS)	Thermal conductivity (W m^{-1} K^{-1})	
	200 wt% alumina to PDMS	300 wt% alumina to PDMS
0.0	0.590	0.855
0.2	0.611	0.884
0.5	0.614	0.891
1.0	0.655	0.931
2.0	0.705	1.004
5.0	0.786	1.142
10.0	0.867	n/a

3. Results and discussion

The composition of the fabricated composites and their measured thermal conductivity are given in Table 1. It is noted that roll milling was impossible for a 10 wt% MWCNT/300 wt% alumina to PDMS content because the compound was too stiff and fragile. Fig. 1 shows the SEM microphotographs of the cryogenically fractured PDMS composite filled with 200 wt% alumina to PDMS and without MWCNT, observed at different magnifications. The critical concentration for percolation of spherical particles in polymer matrices is known to be around 15 vol% [29]. In Fig. 1(a), spherical alumina particles show the dense packing within PDMS. The dense packing of thermally conductive filler in the matrix is very important because it provides the effective pathway for the phonon movement in an insulator. Fig. 1(b) shows the morphology of good wettability between alumina particles and PDMS. This good wettability originates from the hydrogen bonding interaction at the interface. It is well known that metal oxides have abundant hydroxyl groups on their surfaces and these hydroxyl groups can bring about the hydrogen bonding with oxygen atoms in PDMS main chains [30].

Fig. 2 displays the thermal conductivity of the composites filled with 200, 210, and 300 wt% alumina to PDMS and various amounts of MWCNT. The thermal conductivity of the MWCNT incorporated composites was progressively increased with increasing concentration of MWCNT up to 10 wt% to PDMS at the same concentration of alumina. As the thermally conductive filler, alumina increases the thermal conductivity of the composites without the addition of MWCNT. Thermal conductivity of 200, 210 and 300 wt% alumina to PDMS incorporated PDMS was 0.590, 0.623 and 0.855 W m^{-1} K^{-1}, respectively. After the incorporation of MWCNT, the thermal conductivity of the composite shows the high value after 1.0 wt% MWCNT loading relative to PDMS. At 10 wt% MWCNT with 200 wt% alumina to PDMS, the thermal conductivity of the composite was 0.867 W m^{-1} K^{-1}. This value is 47% higher than that of 200 wt% alumina incorporated PDMS. At the same weight of total filler content of 210 wt% to PDMS, the PDMS composite filled with 200 wt% alumina/10 wt% MWCNT to PDMS has a 40% higher thermal conductivity than that of the 210 wt% alumina only filled composite. Bahr et al. reported that the lowering of the percolation threshold when CNT was dispersed together with the insoluble plastic particles in CNT dispersed solution [31]. Both 200 and 300 wt% alumina to PDMS incorporated composites show about 3, 4, 10, 20, and 33% of the thermal conductivity enhancement at 0.2, 0.5, 1, 2, and

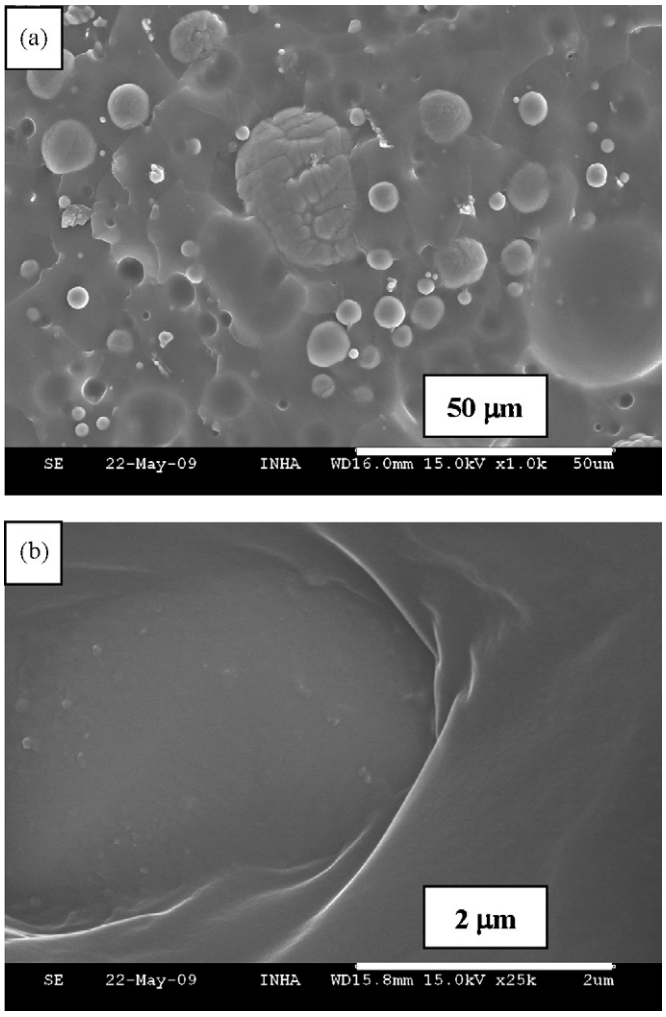

Fig. 1. SEM microphotographs of 200 wt% alumina to PDMS incorporated composite at (a) low and (b) high magnifications.

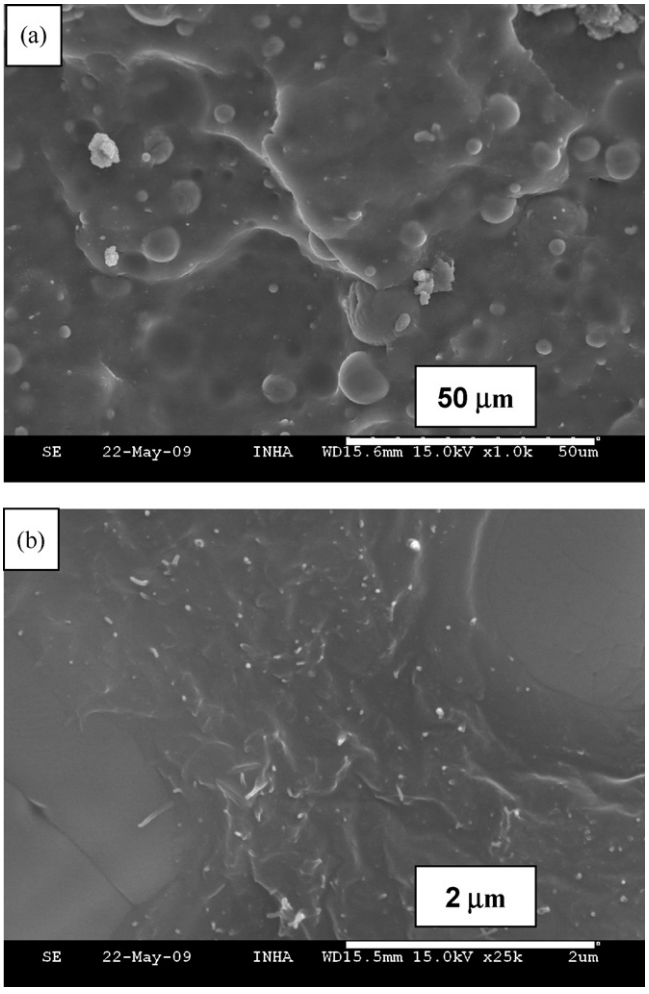

Fig. 3. SEM microphotographs of 200 wt% alumina and 5 wt% MWCNT to PDMS incorporated PDMS at (a) low and (b) high magnifications.

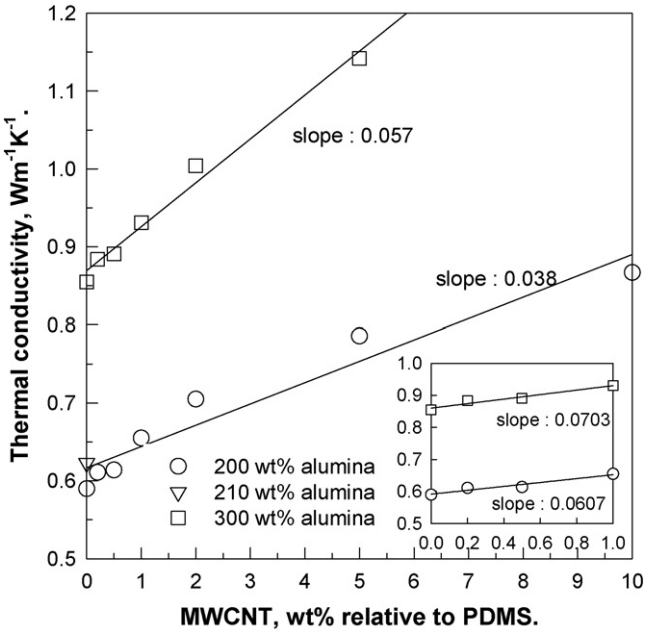

Fig. 2. Thermal conductivity vs MWCNT concentration with 200 wt% (○) 210 wt% (△) and 300 wt% (□) to PDMS–alumina incorporated PDMS. Inset presents the initial slopes at low concentrations of alumina.

5 wt% MWCNT to PDMS incorporation, respectively. For comparing the increase in the thermal conductivity, a simple linear regression was applied. The slope of the composites filled with the 300 wt% alumina to PDMS has a higher value than that of 200 wt% alumina filled systems. The initial slopes (inset to Fig. 2) are much higher because the thermal conductivity of the composite can be increased with the incorporation of small amount of MWCNT. The more alumina particles in the PDMS matrix offer the lower vacancy which can be filled with the PDMS matrix at the same volume. Consequently, MWCNT can easily make the three-dimensional network at the high amount of the alumina and the slope of thermal conductivity as a function of the amount of the MWCNT was higher at 300 wt% alumina to PDMS filled composites than 200 wt% alumina filled composites.

Fig. 3(a) and (b) shows the morphology of the cryogenically fractured composite with 5 wt% MWCNT/200 wt% alumina to PDMS at low and high magnifications, respectively. The composite was soaked in the liquefied nitrogen before the fracture. As shown in Fig. 3, MWCNT between the alumina particles was well-dispersed in the PDMS matrix and it gives a pathway for the heat conduction between the alumina particles existing in PDMS. The viscosity and modulus jumped when the MWCNT was incorporated in the PDMS–alumina composites. Song and Youn showed the rise of complex viscosity at the CNT/epoxy composites [32]. Because the shearing force of the composites is proportional to the viscosity of fluid, fine dispersion of the MWCNT was accomplished during the compounding process. Shimizu et al. reported the fabrication

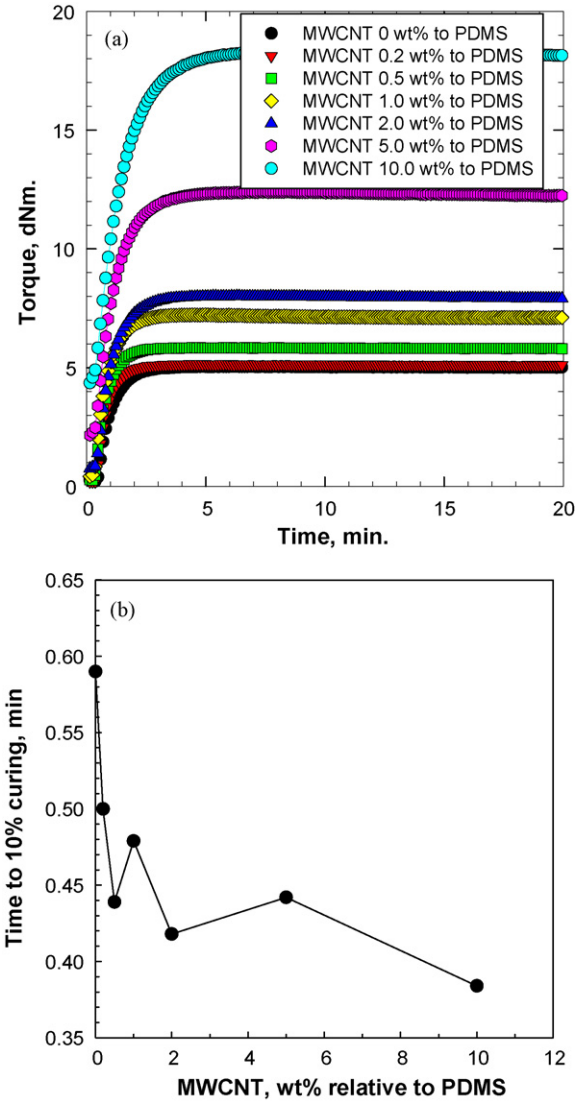

Fig. 4. (a) Cure curves of 0.2, 0.5, 1.0, 2.0, 5.0, and 10.0 wt% MWCNT to PDMS incorporated PDMS containing 200 wt% alumina to PDMS at 170 °C. (b) Scorch time (T′10) vs MWCNT concentration.

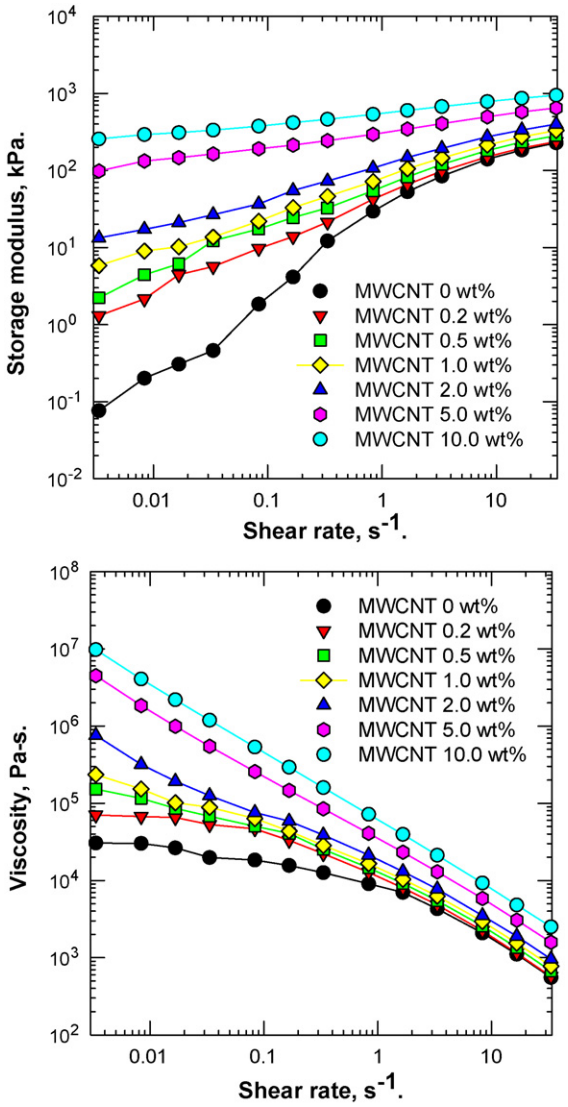

Fig. 5. Storage modulus (top) and complex viscosity (bottom) of MWCNT and 200 wt% alumina to PDMS incorporated PDMS composites with different concentrations of MWCNT.

of homogeneous dispersion of MWCNT in the thermoplastic elastomer via high shear processing [33]. Fig. 3(b) displays the MWCNT dispersion within the PDMS matrix around the alumina particles. Even though MWCNT was incorporated without a prior treatment, the MWCNT in the composite shows the excellent dispersion in the PDMS matrix. The high shear and the ball milling effect from the alumina particles promote the dispersion of MWCNT.

Curing test of the composites containing 200 wt% alumina to PDMS with various amounts of MWCNT was performed using the RPA2000®. In Fig. 4(a), the maximum torque of the composites was proportional to the amount of MWCNT. Especially, the maximum torque jumped above 2.0 wt% MWCNT to PDMS contents, possibly originating from the formation of network structure among MWCNTs. Due to the reinforcing effect of the MWCNT in various polymer-based nanocomposites [34,35], the maximum torque of the composites was naturally increased. In MWCNT and alumina incorporated PDMS nanocomposites, the reversion (the decrease of torque with time) is not observed for prolonged time span because PDMS has excellent thermal stability at a high temperature. Angelini and coworkers reported the reduction of scorch time as increasing amount of MWCNT but there was no clear explanation [35]. In this experiment, the T′10 (the time to achieve 10% cure of the maximum torque) was decreased until the amount of MWCNT reached to 10 wt% to PDMS (Fig. 4(b)). The heat supplied from the surface of the composites can easily penetrate into the center of the composites with enhanced thermal conductivity from the MWCNT loading. Eventually, the crosslinking reaction starts fast, resulting in the reduction in T′10 at the similar maximum torque from 0 to 10 wt% MWCNT to PDMS. At 10 wt% MWCNT incorporation relative to PDMS, the curing reacting instantly starts upon applying heat.

For measuring the dynamic properties of the composites, Rubber Process Analyzer (RPA 2000) with a biconical die containing two cone shaped dies was employed. Fig. 5(a) and (b) shows the storage modulus and complex viscosity, respectively. The rheological properties of the composites were obtained in a frequency sweep mode at 100 °C with 0.2° strain. In Fig. 5(a), the storage modulus of the composites was increased with the increasing MWCNT for the 200 wt% alumina to PDMS incorporated PDMS. Due to the high aspect ratio and surface area of the MWCNT, the composites can easily form the percolated conformation. The filler–filler and filler–fluid interactions are increased with increasing filler contents and the storage modulus increases. For higher than 2 wt% to PDMS loading of MWCNT, the storage modulus of the composites

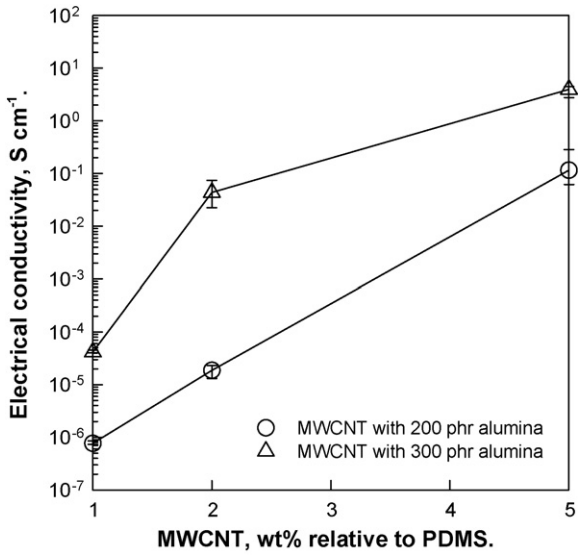

Fig. 6. Electric conductivity of 200 wt% (○) and 300 wt% (△) alumina to PDMS incorporated PDMS composites with different concentrations of MWCNT.

shows a plateau region at low shear rates. This behavior is similar to that of a crosslinked network. The networks from the connection between polymer chain and filler prevent the long range conformational changes and consequently the composite shows the solid like behavior [32,36]. Complex viscosity of the composites as a function of shear rate is displayed in Fig. 5(b). Newtonian behavior in the viscosity is only observed for composites containing MWCNT less than 1.0 wt% to PDMS. Above 1.0 wt% MWCNT to PDMS contents, the PDMS composites filled with alumina and MWCNT exhibit non-Newtonian behavior. 5.0 and 10.0 wt% MWCNT filled PDMS showed the behavior of power law fluids. Similar to the storage modulus, the high aspect ratio and large surface area of MWCNT offer the interactions with the PDMS polymer chains.

The electrical behavior of the composites was explored by measuring the electric conductivity. The electrical conductivity of the MWCNT incorporated polymers has been investigated by many researchers. Winey and Chauver showed the improvement of electrical conductivity for the single walled carbon nanotube (SWCNT)/poly(methyl methacrylate) (PMMA) nanocomposites. The electrical conductivity of the SWCNT/PMMA composite was increased with the small amount of SWCNT (0.5 wt% [37] and 2 vol% [6]) up to about 10^{-1} S m^{-1}. Schulte reported the electrical conductivity of the CNT/epoxy composite using the different types of CNT. The electrical conductivity of the composites was highest at the unmodified CNT [38]. The electrical conductivity of the pure PDMS is 10^{-15} S^{-1} [39]. The electrical conductivity of PDMS was raised up to 10^{-1} S^{-1} at the 4.5 wt% incorporation of carbon black [40]. The electrical conductivity of the alumina/MWCNT incorporated PDMS composites is represented in Fig. 6. The electrical conductivity of the alumina/MWCNT incorporated PDMS composites was dramatically increased with the increment of the amount of MWCNT. In Fig. 6, the electrical conductivity of the composite was higher than 100 S^{-1} (the unit of electrical conductivity is S cm^{-1} in Fig. 6) for 5 wt% MWCNT/300 wt% alumina to PDMS incorporated composite. The higher content of alumina leads the higher electric conductivity at the same concentration of the MWCNT. Considering that alumina is an insulating material, the improved electrical conductivity for higher contents of alumina is ascribed to the fine dispersion of MWCNT in PDMS matrix. With low interstitial area at the high amount of alumina may cause the formation of three-dimensional network of MWCNT, resulting in the significant elevation of electrical conductivity.

4. Conclusion

In order to investigate the effect of electrically insulating particulate filler in PDMS/MWCNT composites, alumina particles were incorporated and their thermal conductivity, dispersion uniformity, rheological properties, curing properties, and electrical conductivity were characterized. The thermal, electrical, and rheological behaviors of the alumina/MWCNT filled PDMS composites were significantly affected with increasing filler concentration. Especially, the thermal and electrical conductivity of the composites were dramatically increased with the increment of MWNCT at high loadings of alumina particles. The SEM morphology showed that MWCNT was finely dispersed throughout the PDMS matrix due to the additional ball milling effect by alumina particles. Although the alumina particles assisted the dispersion MWCNT in PDMS matrix, an abrupt increase in thermal and electrical conductivity was not observed at the low concentration of MWCNT. However, the maximum torque from the curing test, storage modulus, and viscosity of the alumina (200 wt% to PDMS)/MWCNT filled PDMS compounds jumped after 2.0 wt% MWCNT to PDMS loading. It is thought that the addition of electrically insulating hard particles may help disperse MWCNT in PDMS matrix. Finally, the MWCNT/alumina incorporated composites show the high electrical conductivity to the level of the semiconductor.

Acknowledgement

This work was supported by the Korea Science and Engineering Foundation (Grant no. R01-2007-000-20055-0).

References

[1] S.V.N.T. Kuchibhatla, A.S. Karakoti, D. Bera, S. Seal, Prog. Mater. Sci. 52 (2007) 699–913.
[2] X.L. Xie, Y.W. Mai, S.P. Zhou, Mater. Sci. Eng. R 49 (2005) 89–112.
[3] R. Ramasubramaniam, J. Chen, H. Liu, Appl. Phys. Lett. 83 (2003) 2928–2930.
[4] B.B. Parekh, G. Fanchini, G. Eda, M. Chhowalla, Appl. Phys. Lett. 90 (2007) 121913.
[5] R. Viswanath, V. Wakharkar, A. Watwe, V. Lebonheur, Intell. Technol. J. Q3 (2000) 1–7.
[6] P. Bonnet, D. Sireude, B. Garnier, O. Chauvet, Appl. Phys. Lett. 91 (2007) 201910.
[7] C. Lu, Y.W. Mai, J. Mater. Sci. 43 (2008) 6012–6015.
[8] Y. Xu, C.K. Leong, D.D.L. Chung, J. Electron. Mater. 36 (2007) 1181–1187.
[9] M.J. Biercuk, M.C. Llaguno, M. Radosavljevic, J.K. Hyun, A.T. Johnson, Appl. Phys. Lett. 80 (2002) 2767–2769.
[10] M.B. Bryning, D.E. Milkie, M.F. Islam, M. Kikkawa, A.G. Yodh, Appl. Phys. Lett. 87 (2005) 161909.
[11] D.D.L. Chung, Appl. Therm. Eng. 21 (2001) 1593–1605.
[12] L.C. Sim, S.R. Ramanan, H. Ismail, K.N. Seetharamu, T.J. Goh, Thermochim. Acta 430 (2005) 155–165.
[13] W. Zhou, S. Qi, C. Tu, H. Zhao, C. Wang, J. Kou, J. Appl. Polym. Sci. 104 (2007) 1312–1318.
[14] S.H. Kim, S.R. Choi, D. Kim, J. Heat Trans.: Trans. ASME 129 (2007) 298–301.
[15] W. Zhou, S. Qi, Q. An, H. Zhao, N. Liu, Mater. Res. Bull. 42 (2007) 1863–1873.
[16] Q. Mu, S. Feng, G. Diao, Polym. Compos. 28 (2007) 125–130.
[17] B. Lee, J.Z. Liu, B. Sun, C.Y. Shen, G.C. Dai, Express Polym. Lett. 2 (2008) 357–363.
[18] B. Lee, G. Dai, J. Mater. Sci. 44 (2008) 4848–4855.
[19] W. Yu, H. Xie, L. Chen, Y. Li, Thermochim. Acta 491 (2009) 92–96.
[20] I. Yilgor, E. Yilgor, Polym. Bull. 40 (1998) 525–532.
[21] H. Huang, C. Liu, Y. Wu, S. Fan, Adv. Mater. 17 (2005) 1652–1656.
[22] P.C. Song, C.H. Liu, S.S. Fan, Appl. Phys. Lett. 88 (2006) 153111.
[23] W.T. Hong, N.H. Tai, Diam. Relat. Mater. 17 (2008) 1577–1581.
[24] C.H. Liu, S.S. Fan, Appl. Phys. Lett. 86 (2005) 123106.
[25] A. Yu, M.E. Itkis, E. Bekyarova, R.C. Haddon, Appl. Phys. Lett. 89 (2006) 133102.
[26] J. Hong, J. Lee, C.K. Hong, S.E. Shim, Curr. Appl. Phys. 10 (2010) 359–363.
[27] D.S. Bang, H.S. Kye, R.R. Cho, B.G. Min, K.C. Shin, Elastom. Compos. 44 (2009) 22–33.
[28] E.J. Park, J. Lee, D. Jung, S.E. Shim, Elastom. Compos. 45 (2010) 17–24.
[29] R. Pracher, Proc. IEEE 94 (2006) 1571–1586.
[30] S. Takeda, M. Fukuwa, Mater. Sci. Eng. B: Solid 119 (2005) 265–267.
[31] J.C. Grunlan, A.R. Mehrabi, M.V. Bannon, J.L. Bahr, Adv. Mater. 16 (2004) 150–153.
[32] Y.S. Song, J.R. Youn, Carbon 43 (2005) 1378–1385.
[33] Y. Li, H. Shimizu, Polymer 48 (2007) 2203–2207.
[34] M. Moniruzzaman, K.I. Wincy, Macromolecules 39 (2006) 5194–5205.

[35] F. Cataldo, O. Ursini, G. Angelini, Fullerene Nanotubes Carbon Nanostruct. 17 (2009) 38–54.
[36] S.E. Shim, A.I. Isayav, Rheol. Acta 43 (2004) 127–136.
[37] F. Du, C. Guthy, T. Kashiwagi, J.E. Fischer, K.I. Winey, J. Polym. Sci. Part B: Polym. Phys. 44 (2006) 1513–1519.
[38] F.H. Gojny, M.H.G. Wichmann, B. Fiedler, I.A. Kinloch, W. Bauhofer, A.H. Windle, K. Schulte, Polymer 47 (2006) 2036–2045.
[39] A.T. Nicholson, S.N. Jayasinghe, Biomacromolecules 7 (2006) 3364–3369.
[40] M. Kontopoulou, M. Kaufman, A. Docoslis, Rheol. Acta 48 (2009) 409–421.